SUPPLEMENTAL INFORMATION

SUPPLEMENTAL FIGURES

SUPPLEMENTAL TABLES

SUPPLEMENTAL EXPERIMENTAL PROCEDURES

SUPPLEMENTAL REFERENCES

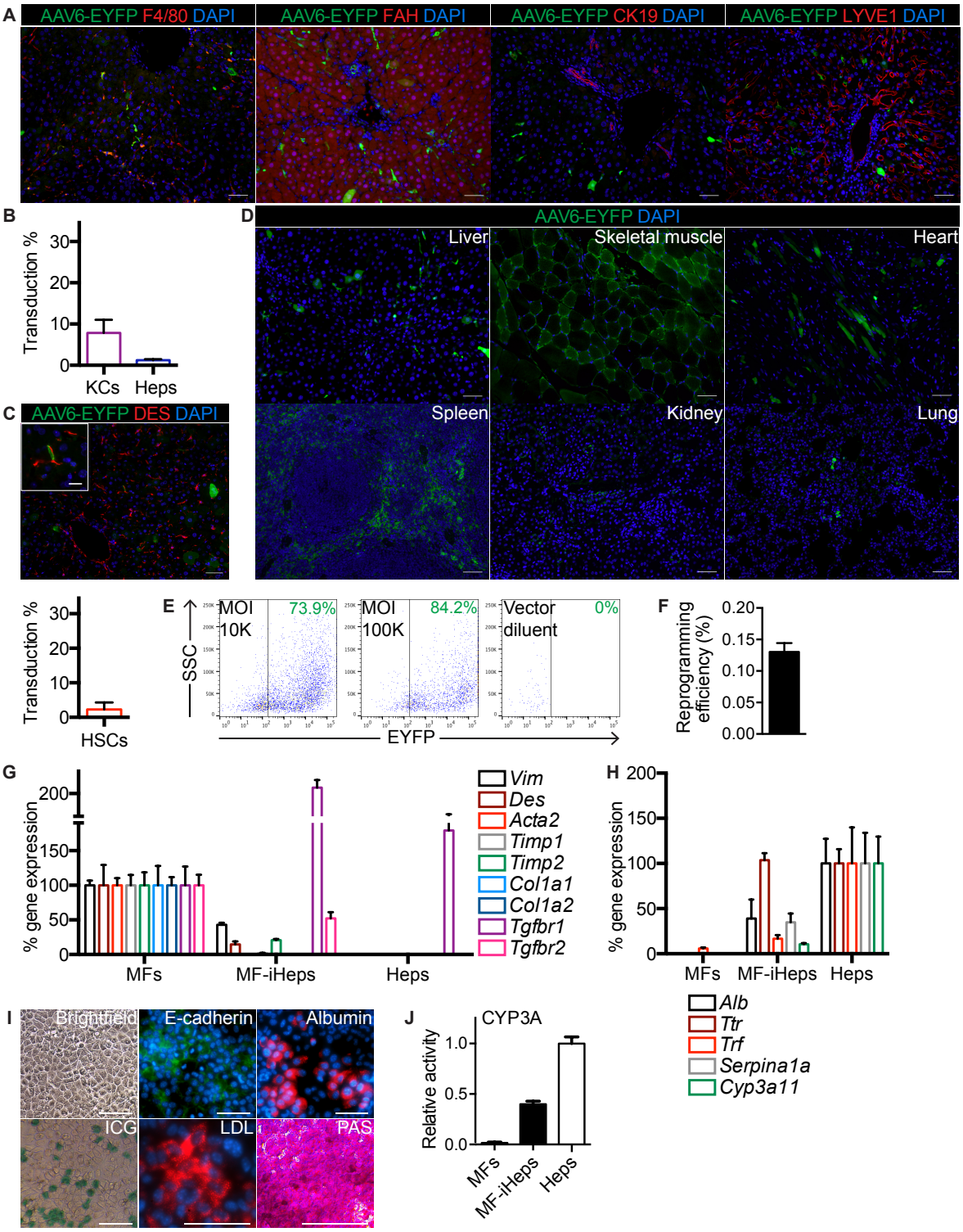

Figure S1 (related to Figure 1). MF Gene Delivery and Reprogramming Tools

(A-D) Liver cell and organ tropism of AAV6.

(A) EYFP and F4/80 (Kupffer cells), FAH (hepatocytes), CK19 (cholangiocytes) or LYVE1 (endothelial cells) co-IF of livers of recipients of AAV6-EYFP. Size bars, 50 µm.

(B) Quantification of Kupffer cells (KCs) and hepatocytes (Heps) transduced by AAV6-EYFP. Results are means ± SD for biological replicates (n = 2).

(C) EYFP and DES co-IF of liver of mouse intravenously injected with 4 x 10^{11} viral genomes of AAV6-EYFP but not treated with CCl4. Size bars, 50 µm and 15 µm (inset). Plot shows quantification of DES-positive quiescent hepatic stellate cells (HSCs) transduced by AAV6-EYFP. Results are means ± SD for biological replicates (n = 3).
(D) EYFP IF of other organs of AAV6-EYFP recipients. Size bars, 50 µm.
(E-J) In vitro hepatic reprogramming of MFs with AAV6-6TFs.
(E) Quantification by flow cytometry of MFs transduced in vitro by AAV6-EYFP at different multiplicity of infection (MOI). MFs treated with vector diluent were used as EYFP-negative control.
(F) Quantification of expandable iHep colonies generated by transduction of MFs with AAV6-6TFs. Results are means ± SD for biological replicates (n = 2).
(G,H) qRT-PCR analysis of genes reflecting MF (G) or hepatocyte (H) differentiation in MF-iHeps relative to MFs and primary hepatocytes (Heps). Results are means for technical replicates (n = 3).
(I) Assessment of hepatocyte function of MF-iHeps by IF and analysis of indocyanine green (ICG) or low-density lipoprotein (LDL) uptake and glycogen storage using Periodic acid-Schiff (PAS) staining. Size bars, 50 µm.
(J) CYP3A (includes CYP3A11, the mouse CYP enzyme that corresponds to human CYP3A4) activity of MF-iHeps relative to MFs and primary hepatocytes (Heps). Results are means ± SD for technical replicates (n = 3).

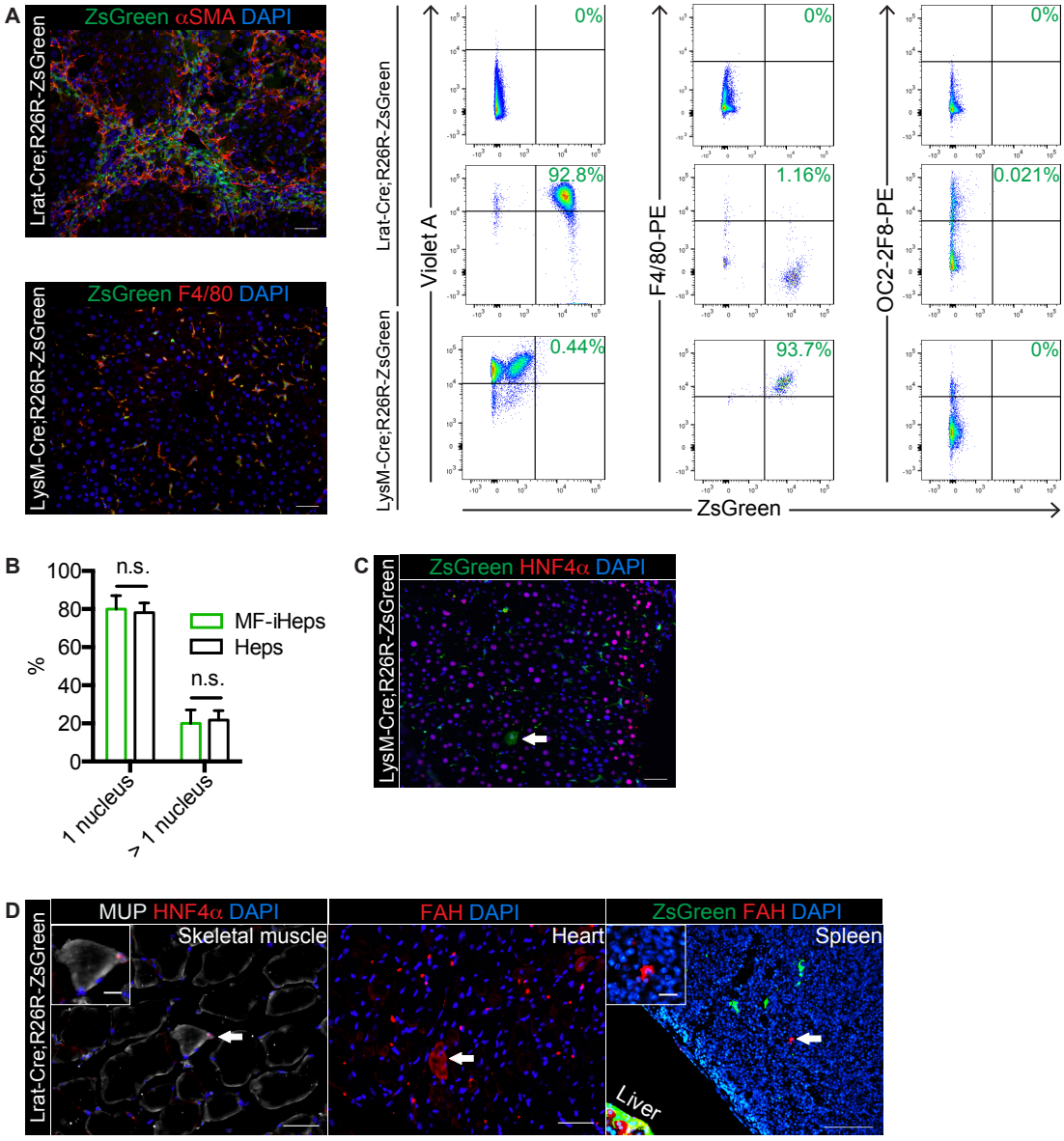

Figure S2 (related to Figure 2). Specificity of In Vivo Hepatic Reprogramming of MFs

(A) Specificity and efficiency of MF and Kupffer cell fate tracing in Lrat-Cre;R26R-ZsGreen and LysM-Cre;R26R-ZsGreen mice treated with 12 doses of CCl4. ZsGreen fluorescence and αSMA or F4/80 IF of livers. Size bars, 50 μm. Quantification by flow cytometry of ZsGreen-expressing vitamin A (Violet A)-positive or F4/80-positive nonparenchymal liver cells and OC2-2F8-positive hepatocytes. Unstained wildtype cells were used to set up gating; MFs were bleached with UV. Results are representative of biological replicates (n = 2).

(B) Quantification of nuclei in newly formed MF-iHeps and surrounding primary hepatocytes (Heps) excludes cell fusion as the mechanism of MF-iHep formation because initial fusion products frequently contain two nuclei (Willenbring et al., 2004). Results are means ± SEM for biological replicates (n = 4). Student's *t* test; n.s., not significant.

(C) ZsGreen fluorescence and HNF4α IF of liver of an LysM-Cre;R26R-ZsGreen mouse treated with the CCl4 stop protocol. Arrow points at rare double-positive cell. Size bar, 50 μm. Result is representative of biological replicates (n = 3).

(D) MUP and HNF4α co-IF of skeletal muscle and FAH IF of heart and spleen from Lrat-Cre;R26R-ZsGreen mice treated with the CCl4 stop protocol. Size bars, 50 μm. Arrows and insets highlight rare cells expressing hepatocyte markers. Results are representative of biological replicates (n = 6).

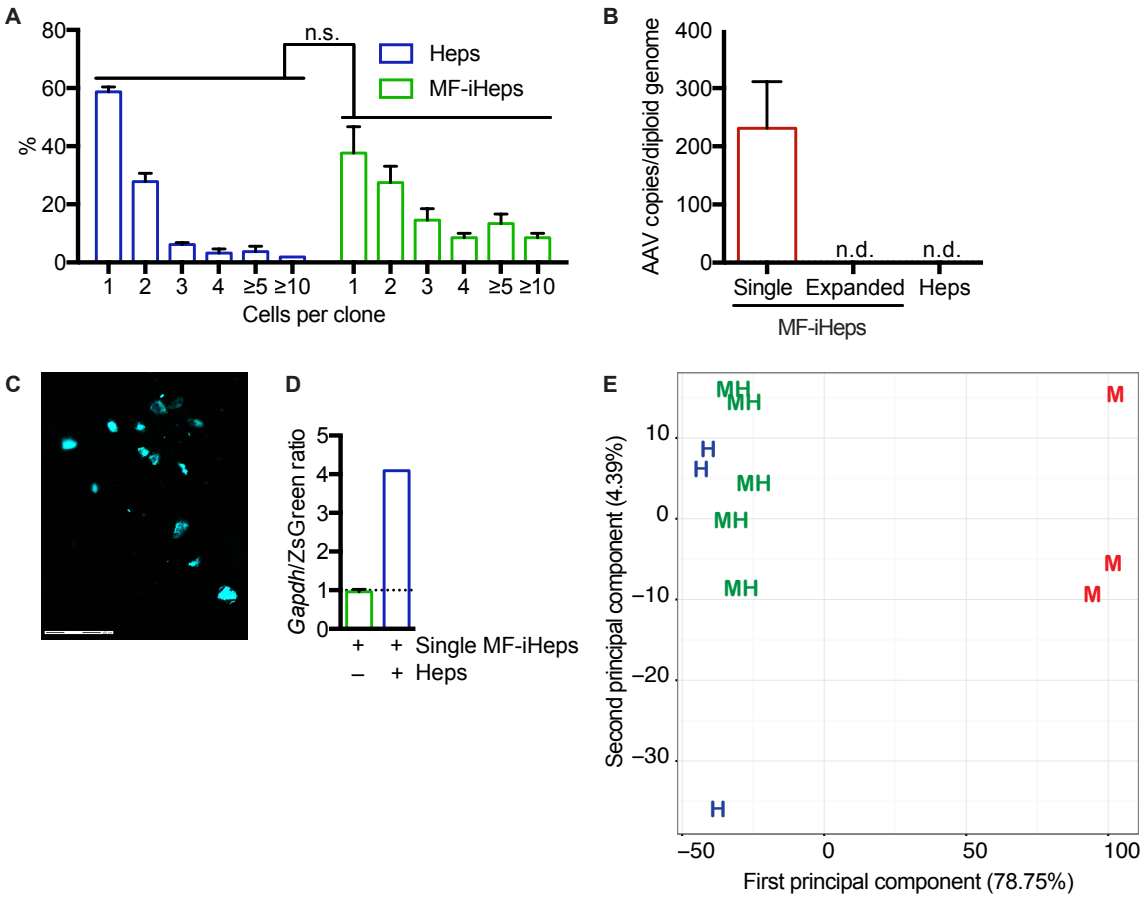

Figure S3 (related to Figure 3). MF-iHep Proliferation and Differentiation

(A) Quantification of clonal expansion of MF-iHeps and primary hepatocytes (Heps). Results are means ± SEM for biological replicates (n = 3). Multiple Student's *t* test; n.s., not significant.

(B) Analysis of AAV vector copy number in MF-iHeps by CMV promoter qPCR. Single MF-iHeps were isolated by LCM from Lrat-Cre;R26R-ZsGreen mice treated with the CCl4 stop protocol. Clonally expanded MF-iHeps were isolated from Lrat-Cre;R26R-ZsGreen mice treated with the recurring CCl4 protocol. Primary hepatocytes (Heps) were located in proximity to single MF-iHeps. Pooled LCM samples were analyzed in replicates (n = 6 for single MF-iHeps, n = 2 for clonally expanded MF-iHeps, n = 2 for Heps). Results are means ± SEM for biological replicates. n.d., not detected.

(C) Image of dissected single ZsGreen-positive MF-iHeps in cap of LCM collection tube. Size bar, 150 μm.

(D) Accuracy of single MF-iHep isolation by LCM illustrated by the ratio of ZsGreen to *Gapdh* gene expression measured by qRT-PCR. MF-iHeps express ZsGreen and *Gapdh* at similar levels; primary hepatocytes (Heps) express *Gapdh* but not ZsGreen. Dissected single MF-iHeps have a *Gapdh*/ZsGreen ratio of about 1; a dissectant including single MF-iHeps and contaminating primary hepatocytes has a higher ratio in favor of *Gapdh*.

(E) 2D principal component analysis of the 10,000 most highly expressed genes in the global gene expression profiling (MF-iHeps, MH; primary hepatocytes, H; MFs, M).

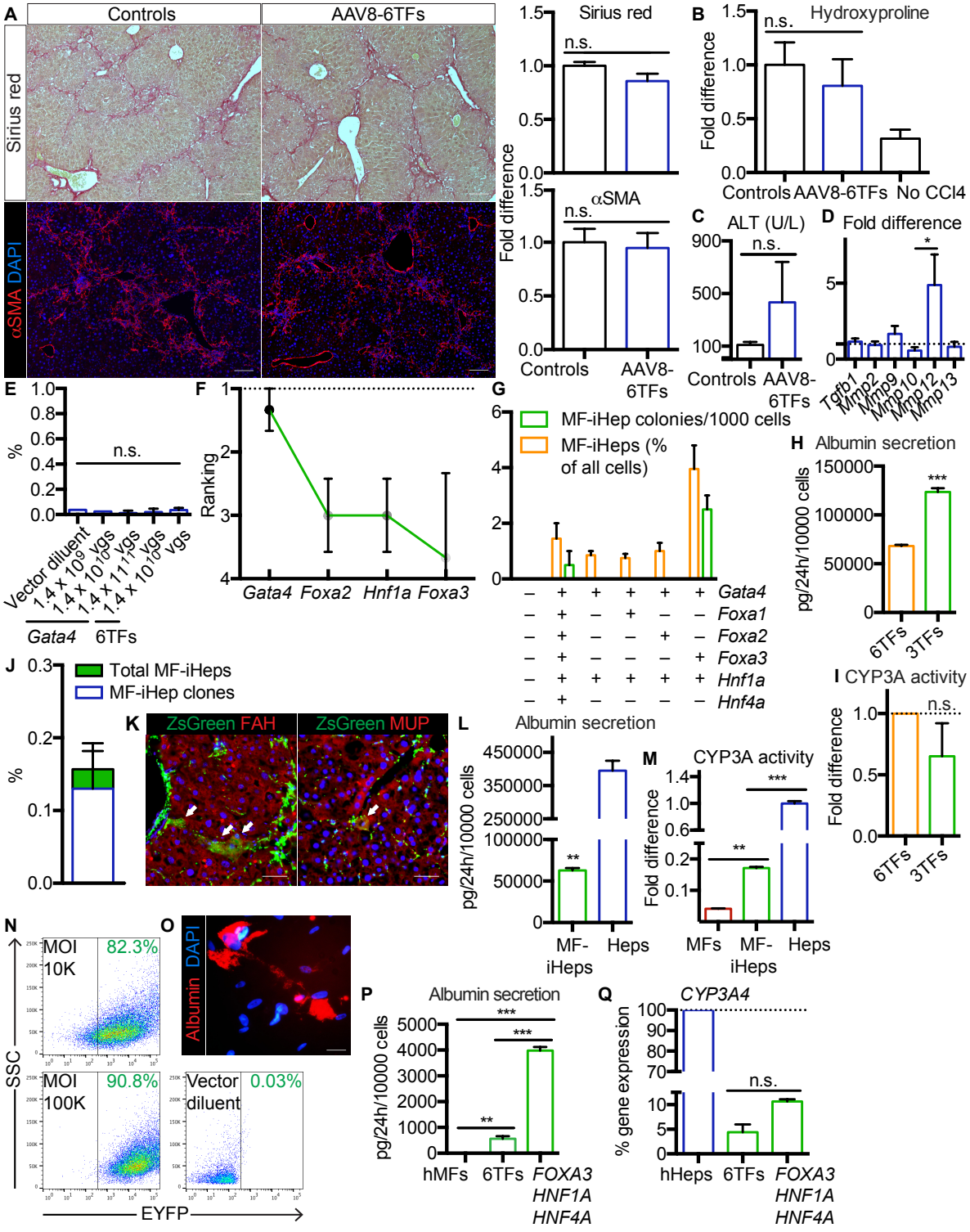

Figure S4 (related to Figure 4). Mechanistic Studies and Further Development of In Vivo Hepatic Reprogramming of MFs

(A-D) Contribution of expression in hepatocytes to therapeutic efficacy of AAV6-6TFs.

(A) Sirius red staining and αSMA IF with quantification. Size bars, 100 μm. Results are means ± SEM for biological replicates (n = 3). Student's *t* test; n.s., not significant.

(B) Analysis of whole liver collagen content by hydroxyproline assay. Results are means ± SEM for biological replicates (n = 3). Student's *t* test; n.s., not significant.
(C) Serum levels of ALT. Results are means ± SEM for biological replicates (n = 3). Student's *t* test; n.s., not significant.
(D) Whole liver gene expression analysis by qRT-PCR. Results are means ± SEM for biological replicates (n = 3). Ordinary one-way ANOVA; multiple comparisons; $*P < 0.05$; all other comparisons not significant.
(E) Exclusion of unspecific activation of MF fate tracing in hepatocytes of Lrat-Cre;R26R-ZsGreen mice. Because *Gata4* is more highly expressed in MFs than in primary hepatocytes (Table S1), activation of the reporter in hepatocytes by AAV-mediated exogenous *Gata4* expression was excluded by intravenously injecting Lrat-Cre;R26R-ZsGreen mice treated with the CCl4 stop protocol with 1.4×10^9, 1.4×10^{10} or 1.4×10^{11} viral genomes (vgs) of AAV8-*Gata4* (*Gata4*), thereby transducing 1%, 10% or > 70% of all hepatocytes in the liver (Table S2). AAV8-6TFs (6TFs) containing *Gata4* and five TFs normally expressed in primary hepatocytes were intravenously injected at a dose of 1.4×10^{10} vgs. Vector diluent was used as negative control. Results are means ± SEM for biological replicates (n = 2, 1, 2, 2, 2 from vector diluent to AAV8-6TFs). Ordinary one-way ANOVA; multiple comparisons; n.s., not significant.
(F-M) Essential TF combination.
(F) Analysis of AAV6-TF enrichment by qRT-PCR of each of the six exogenous TF genes in newly formed single MF-iHeps isolated by LCM from mice treated with the CCl4 stop protocol. Ranking results are means ± SEM for biological replicates (n = 3). The top four AAV6-TFs are shown (1, most enriched).
(G) In vitro validation of TF combinations suggested by the in vivo enrichment analysis by analysis of efficiency of hepatic reprogramming of MFs isolated from Lrat-Cre;R26R-ZsGreen mice and formation of MF-iHep colonies (> 4 cells). MF-iHeps were identified by ZsGreen fluorescence and albumin IF (data not shown). Results are means ± SEM for biological replicates (n = 2).
(H, I) Comparison of albumin secretion (H) and CYP3A activity (I) between MF-iHeps generated in vitro with AAV6-6TFs (6TFs) or AAV6 vectors expressing *Foxa3*, *Gata4* and *Hnf1a* (3TFs). Results are means ± SEM for biological replicates (n = 4 for 6TFs and n = 2 for 3TFs). Student's *t* test; $***P < 0.001$; n.s., not significant.
(J) In vivo hepatic reprogramming efficiency and liver repopulation assessed by quantification of MF-iHep clones and total MF-iHeps, respectively, in Lrat-Cre;R26R-ZsGreen mice treated with the CCl4 stop protocol using AAV6-3TFs. Results are means ± SEM for biological replicates (n = 3).
(K) ZsGreen fluorescence and FAH or MUP IF of livers of mice treated with the CCl4 stop protocol using AAV6-3TFs. Nuclei are stained blue with DAPI. Arrows point at MF-iHeps. Size bars, 50 μm.
(L, M) Analysis of albumin secretion (L) and CYP3A activity (M) in MF-iHeps generated with AAV6-3TFs, primary hepatocytes (Heps; same as in Figure 3D) and MFs. All cells were isolated from Lrat-Cre;R26R-ZsGreen mice by FACS. Results are means ± SEM for biological replicates (n = 2). Student's *t* test; $**P < 0.01$; $***P < 0.001$.
(N-Q) Efficient transduction and hepatic reprogramming of primary human MFs with AAV6 vectors in vitro.
(N) Quantification by flow cytometry of human MFs (hMFs) transduced in vitro with AAV6-EYFP at different MOI. hMFs treated with vector diluent were used as EYFP-negative control.
(O) Albumin IF illustrating formation of 3.5% ± 0.71% albumin-positive cells after transduction of hMFs with AAV6-6TFs at MOI 100K. Result is means ± SD for biological replicates (n = 4). Size bar, 15 μm.
(P, Q) Comparison of albumin secretion (P) and *CYP3A4* gene expression (Q) between hMF-iHeps generated in vitro with AAV6-6TFs (6TFs) or AAV6 vectors expressing *FOXA3*, *HNF1A* and *HNF4A*, a TF combination previously reported to be effective in generating iHeps from human skin fibroblasts (Huang et al., 2014). Results are means ± SEM for biological replicates (n = 3). Student's *t* test; $**P < 0.01$; $***P < 0.001$; n.s., not significant.

SUPPLEMENTAL TABLES

Table S1 (related to Figure 3). Differential Gene Expression Including Pathway Analysis

Table S2 (related to Figure 4). AAV8 Dose Finding

SUPPLEMENTAL EXPERIMENTAL PROCEDURES

AAV-Capsid Vector Construction

AAV helper plasmids (pAAV-capsid) co-expressing the *rep* gene from AAV2 and *cap* genes from AAV1, AAV2, AAV5, AAV6 and AAV9 and the AAV2/8/9 chimera AAV-DJ have been reported (Grimm et al., 2008). A helper plasmid for the production of the AAV1P4 (Borner et al., 2013) vector was created through PCR-based introduction of two unique SfiI restriction sites into the AAV1 *cap* gene and subsequent insertion of a double-stranded DNA oligonucleotide encoding a seven amino acid re-targeting peptide (P4). A helper plasmid for the production of the AAV2(Y444,500,730F) vector was created by three rounds of site-directed mutagenesis using the QuickChange II Kit (Stratagene) as in the original report of this triple tyrosine-to-phenylalanine mutant (Li et al., 2010).

AAV-TF Vector Construction

Transcription factor (TF) cDNAs were derived from Gateway-compatible plasmids (GeneCopoeia): *Foxa1*: GC-Mm03068, *Foxa2*: GC-Mm30428, *Foxa3*: GC-Mm03070, *Gata4*: GC-Mm02662, *Hnf1a*: GC-Mm21209 and *Hnf4a*: GC-Mm03071. *Hnf1a*, *Foxa3* and *Gata4* cDNAs were inserted into the single-stranded AAV vector backbone plasmid pAAV-CMV-Gateway (Applied Viromics) by LR reaction using Gateway LR Clonase enzyme mix (Life Technologies). *Foxa1*, *Foxa2* and *Hnf4a* cDNAs were inserted into a modified version of the double-stranded (DS) plasmid pAAV-CMV-EYFP-U6/DS (bi-cistronic AAV vector backbone containing a CMV promoter-driven EYFP and a U6 promoter for shRNA expression) in which the U6 promoter was deleted by XhoI/AscI (New England Biolabs) digestion. *Foxa1*, *Foxa2* and *Hnf4a* cDNAs were amplified by PCR from GeneCopoeia plasmids and AgeI and SalI restriction sites were added in 5' and 3', respectively, for subsequent insertion into pAAV-CMV-EYFP/DS. All plasmids were sequenced after amplification using the EndoFree Plasmid Mega Kit (Qiagen). Sequence-validated plasmids were functionally validated by transfection of 2 μg plasmid into HEK293T cells (Agilent Technologies) using 1 μL MegaTran transfection reagent (Origene) followed by RNA isolation for qRT-PCR analysis of TF expression 48 hours later (data not shown). Mycoplasma contamination was ruled out using the MycoAlert Detection Kit (Lonza).

AAV Vector Production

AAV vectors were produced by transfecting HEK293T cells in 20 15-cm dishes with a combination of 3 plasmids—pAAV-CMV-EYFP-U6/DS or pAAV-CMV-TF, adenoviral helper plasmid pVAE2AE4-5 (Matsushita et al., 1998) and pAAV-capsid—using the calcium phosphate method (Grimm et al., 2006). Virus was harvested 3 days after transfection.

AAV Vector Purification

HEK293T cells were lysed by 5 cycles of freezing (-196°C) and thawing (37°C) and sonicated for 1 minute and 20 seconds. Samples were digested with benzonase (EMD Millipore) at 50 U/mL for 1 hour at 37°C and centrifuged at 5,000 g for 15 minutes at 4°C. Viral particles were purified using an iodixanol (Sigma-Aldrich) density gradient (Zolotukhin et al., 1999). In a 29.9 mL OptiSeal Tube (Beckman-Coulter), the crude virus and gradient were loaded as follows: 8 mL crude virus, 7 mL 15% iodixanol, 5 mL 25% iodixanol, 4 mL 40% iodixanol and 4 mL 60% iodixanol. Samples were centrifuged for 2.5 hours at 250,000 g at 4°C in a 70 Ti rotor using an Optima L-90K ultracentrifuge (Beckman-Coulter). After ultracentrifugation, viral particles accumulating in the 40% phase of the iodixanol gradient were eluted by aspiration of the phase. AAV vector titers were determined by qPCR as previously described (Malato et al., 2011).

Tissue Immunofluorescence and Staining

Tissue samples were fixed in 10% formalin (Sigma-Aldrich) at 4ºC overnight. After storage in 70% ethanol and paraffin embedding, tissues were cut into 5-μm sections and placed on Superfrost Plus slides (Fisher Scientific). Sections were deparaffinized and incubated in boiling TRIS or TRIS-EDTA buffer for 20 minutes. After cooling down, sections were blocked in 1% bovine serum albumin (BSA; Sigma-Aldrich) for 30 minutes and incubated with primary antibodies overnight at 4°C and secondary antibodies for 1 hour at room temperature. Nuclear DNA was stained with 300 nM DAPI (Millipore). To generate cryosections, samples were fixed in 4% paraformaldehyde for 2 hours at room temperature and cryoprotected in 30% sucrose (Sigma-Aldrich) at 4ºC overnight before embedding and freezing in optimum cutting temperature compound (OCT; Tissue-Tek, Sakura Finetek). Frozen tissues were cut into 5-10-μm sections using a Leica 3050S Cryostat, air dried and stored at -20ºC prior to antibody staining. For Sirius red staining a standard protocol was used (Junqueira et al., 1979). Images were captured using an Olympus BX51 microscope coupled to a QImaging Retiga 2000R camera. Quantification was done using NIH-ImageJ

software to analyze 6 to 10 random images at 10x magnification from ≥3 liver sections obtained from 3 different liver lobes per mouse.

Laser-Capture Microdissection to Microarray and qRT-PCR

MF-iHeps in 7-µm cryosections of unfixed, OCT-embedded liver samples from Lrat-Cre;ZsGreen mice were isolated by laser-capture microdissection (LCM) using a PALM MicroBeam IV system (Zeiss) as previously described (Zhu et al., 2014). A range of 25-82 MF-iHeps were pooled per sample. Control hepatocytes were isolated from the same mice. MFs were isolated by FACS from littermates receiving the same CCl4 treatment. RNA was extracted with the Arcturus Pico Pure RNA Isolation Kit (AB Biosystems). Total RNA (0.4 to 1.0 ng) was reverse transcribed, amplified and biotin labeled using the Ovation Pico WTA System V2 and the Encore Biotin Module (NuGEN Technologies). Labeled cDNA targets were hybridized to GeneChip Mouse Gene 1.0 ST arrays (Affymetrix). Images were processed using Affymetrix Command Console v.3.1.1 software and expression analysis for QC was performed using Affymetrix Expression Console v.1.4 software with normalization by Robust Multi-Array Average (RMA). For statistical analyses, all array probesets were removed where no experimental groups had an average log2 intensity greater than 3.0. Linear models were fitted for each gene using the bioconductor limma package in R. Moderated *t* statistics, fold change and the associated *P* values were calculated for each gene. Samples and genes were hierarchically clustered using the default R function hclust. Heatmaps were generated using heatmap.2 in the gplots suite (http://cran.r-project.org/web/packages/gplots/index.html). Genes for heatmaps reflecting hepatocyte (Huang et al., 2011; Peng et al., 2012; Tarlow et al., 2014) or MF/HSC (Duarte et al., 2015; Hayes et al., 2014; Henderson et al., 2013; Iwaisako et al., 2014; Lua et al., 2016; Mederacke et al., 2013; Schuppan et al., 2001) differentiation were derived from the literature. Microarray experiments were performed in the Gene Profiling Shared Resource at Oregon Health & Science University. Differential gene expression analysis, principal component analysis, hierarchical clustering and heatmap illustration were done in the Gladstone Bioinformatics Core. Microarray results for genes reflecting hepatocyte and MF/HSC differentiation were confirmed by qRT-PCR analysis. First-strand reverse transcription was performed with 4 ng of RNA using the qScript cDNA synthesis kit (Quanta). qPCR was performed using VeriQuest Fast SYBR qPCR Master Mix (Affymetrix) on an Applied Biosciences ViiA 7 Real-Time PCR system (Life Technologies).

Hydroxyproline Assay

Snap-frozen mouse liver samples were homogenized in distilled water and after adding equal amounts of concentrated (12N) hydrogen chloride (Sigma-Aldrich) hydrolyzed at 120°C for 3.5 hours. Hydroxyproline content was quantified using a colorimetric assay (Hydroxyproline Assay Kit, Biovision). Fibrotic liver from CCl4-treated mice and rat collagen (9.37 mg/mL; Corning) were used as positive controls. Sample concentrations were normalized to input liver sample weight.

Serum Analysis

Peripheral blood was obtained by retro-orbital venipuncture. ALT was analyzed on an ADVIA 1800 automated clinical chemistry system (Siemens). For serum separation blood was centrifuged in 1.1 mL Z-gel micro tubes (Sarstedt) at 10,000 g for 5 minutes at room temperature.

Hepatocyte Isolation

Single-cell suspensions of hepatocytes were isolated by perfusion through a 24-gauge intraportal catheter with Liver Perfusion Medium (LPM) followed by Liver Digest Medium (both Life Technologies). Hepatocytes released from the liver were filtered through a 40-µm cell strainer (BD Falcon) and centrifuged twice at 100 g in DMEM (UCSF Cell Culture Facility)/5% FBS (Gemini Bio-Products). To enrich viable hepatocytes to ~95%, cells were layered on top of 50% DMEM/F12 medium (Life Technologies)/Percoll solution (Sigma-Aldrich) and centrifuged at 200 g. Cell viability was assessed by trypan blue (Sigma-Aldrich) staining.

FACS

Freshly isolated hepatocytes were resuspended in Hanks' BSS (Life Technologies)/10% FBS before incubation with anti-CD16/CD32 antibody for 20 minutes and PE-conjugated anti-CD31 antibody for 60 minutes on ice. After being washed in PBS, cells were resuspended in phenol-free Williams E medium (Sigma-Aldrich)/2% FBS. Sytox Red was used to label dead cells. ZsGreen-positive MF-iHeps and ZsGreen-negative primary hepatocytes were analyzed and sorted after gating out doublets and vitamin A (Violet A)-positive HSCs/MFs and CD31-positive endothelial cells on a MoFlo XDP (150 µm nozzle, 15 psi sheath pressure, 21,460 Hz drop drive frequency; Beckman-Coulter).

ZsGreen signal specificity was established using hepatocytes from wildtype mice as negative control and Violet A-positive HSCs from Lrat-Cre;R26R-ZsGreen mice as positive control.

Albumin ELISA
Enzyme-linked immunoabsorbent assay (ELISA) kits for the detection of mouse (Bethyl E90-134) and human (Bethyl E80-129) albumin in cell culture medium were used according to the manufacturer's instructions. FACS-isolated MF-iHeps were analyzed 24 hours after plating.

Cytochrome P450 Assay
The CYP3A4 P450-Glo Assay with Luciferin-IPA (Promega) was used to measure CYP3A activity 90 minutes after substrate exposure using a Synergy 2 plate reader (BioTek) (Roncoroni et al., 2012). Cell viability was assessed by trypan blue (Sigma-Aldrich) staining. FACS-isolated MF-iHeps were analyzed 24 hours after plating.

Urea Production Assay
The QuantiChrom Urea Assay Kit (BioAssay Systems) was used according to the manufacturer's instructions to measure urea production by FACS-isolated MF-iHeps after 24 hours of cell culture.

Exclusion of Cell Fusion
The number of nuclei in newly formed MF-iHeps and surrounding primary hepatocytes was determined in 10-µm-thick liver sections from mice treated with the CCl4 stop protocol.

AAV Genome Detection
Single or clonally expanded MF-iHeps in Lrat-Cre;R26R-ZsGreen mice treated with the CCl4 stop protocol or recurring CCl4 protocol, respectively, were identified by direct fluorescence and isolated by LCM. Primary hepatocytes located in the proximity of single MF-iHeps were also isolated by LCM. Single MF-iHep samples consisted of 10-22 cells. Expanded MF-iHep samples consisted of 14 MF-iHep nodules, each containing ≥ 10 cells. Primary hepatocyte samples consisted of 10-33 cells. DNA was extracted using the Arcturus Pico Pure DNA Extraction Kit (Life Technologies) and analyzed by qPCR using primers specific for the CMV promoter in the AAV vector. Standard curves were generated from serial dilutions of AAV vector backbone plasmid and genomic DNA from wildtype mice. Diploid genomes were calculated based on an estimate of 3 pg DNA per haploid and 6 pg DNA per diploid genome. *Gapdh* was amplified in all samples to ascertain presence of genomic DNA.

Nonparenchymal Liver Cell Isolation
Primary nonparenchymal liver cells were isolated by pronase/collagenase liver perfusion as previously reported (Mederacke et al., 2015).

Hepatic Stellate Cell Isolation
Primary hepatic stellate cells (HSCs) were isolated by pronase/collagenase liver perfusion. Mice were anesthetized with vaporized isoflurane. The superior vena cava was canulated using a 24-gauge catheter (Surflo, Terumo). Liver perfusion was started with LPM (5 mL/minute) and the portal vein was cut for drainage. Pronase/collagenase solutions were prepared using DMEM/F12 medium (Life Technologies). After perfusion with LPM for 3 minutes, the liver was perfused with 14 mL of high-pronase solution (from *Streptomyces griseus*, Roche) at 1.14 g/L, followed by perfusion with 42 mL of collagenase solution (crude, Crescent Chemical) at 0.15 g/L for 10 minutes. The liver was removed from the mouse after complete digestion, placed into a 100-mm petri dish containing warmed 2.5 mL of DNase solution at 0.08 g/L, minced using sharp scissors and transferred into a bottle containing warmed low-pronase/collagenase solution at 0.25 g/L of pronase and 0.08 g/L of collagenase. The petri dish was rinsed with warm DMEM/F12, which was added to the low-pronase solution containing the minced liver. The volume was adjusted to 25 mL using warm DMEM/F12. The cell suspension was mixed at 37°C using a shaking water bath for 10 minutes. After two washes at 10°C and 600 g, the cell suspension was purified by discontinuous density-gradient centrifugation as previously reported (Mederacke et al., 2015). HSCs were collected, washed twice in DMEM/F12 and used for RNA extraction and cell culture.

Hepatic Stellate Cell Culture
Primary HSCs were plated on 6-well plastic dishes (Corning) immediately after isolation and maintained in DMEM/F12/10% FBS, 1% Glutamax (Life Technologies) and 1% antibiotic/antimycotic solution (Gemini Bio-

Products) at 37°C in 5% CO_2. Myofibroblasts (MFs) were generated by in vitro activation of HSCs by culture for 10 days. MFs were transduced in FBS-free medium and analyzed 48 hours later.

In Vitro Hepatic Reprogramming of Mouse and Human MFs

5 x 10^4 in vitro activated primary mouse MFs were transduced after 2 passages in FBS-free DMEM/F12 with AAV6-6TFs (MOI 5 x 10^5 each). Transduction with AAV6-EYFP was carried out as a control. 24 hours after transduction, cells were washed once with PBS and cultured in DMEM/F12/5% FBS for 4 days. At day 5, cells were changed to medium previously used to generate iHeps from mouse fibroblasts (Sekiya and Suzuki, 2011), consisting of DMEM/F12/10% FBS supplemented with 1 µg/mL insulin (Sigma-Aldrich), 0.1 µM dexamethasone (Sigma-Aldrich), 10 mM nicotinamide (Sigma-Aldrich), 2 mM L-glutamine, 50 µM β-mercaptoethanol (Gibco), 1% penicillin/streptomycin (Gibco), 20 ng/mL hepatocyte growth factor and 20 ng/mL epidermal growth factor (both Peprotech). At day 14-16, epithelial colonies were isolated by applying Accutase (Gibco) directly to the colonies and transferred to collagen I (Corning)-coated 96-well plates (Corning) for expansion. At 90% confluency, cells were serially passaged into the next larger plate format. After passaging into a 12-well plate (day 40-45), cells were cultured for 7-10 days in hepatocyte maturation medium previously used for culturing human iPSC-derived hepatocytes (Ware et al., 2015) but modified to exclude oncostatin M. The medium consisted of RPMI (Gibco), 1 µM dexamethasone, 2% B27 (Gibco) and 1% penicillin/streptomycin. To generate human MF-iHeps, primary human HSCs (ScienceCell Research Laboratories; catalog # 5300, lot # 10744) were expanded and activated on plastic for 14-16 days and, after seeding on collagen I (Corning)-coated 6-well-plates, transduced in FBS-free DMEM/F12 for 24 hours at MOI 1 x 10^5 with the AAV6 vectors used for mouse cell reprogramming. Transduced cells were kept in DMEM/F12/10% FBS for a week before they were changed to maturation medium for another week, consisting of IMDM (Gibco) supplemented with B27 with insulin (Gem21/Neuroplex, Gemini Bio-Products), 2 mM L-glutamine, 0.126 U/mL human insulin (Sigma-Aldrich), 0.1 µM dexamethasone, monothioglycerol (21.6 µL in 500 mL; Sigma-Aldrich), 1x nonessential amino acids (Gibco), 20 ng/mL hepatocyte growth factor, 20 ng/mL epidermal growth factor (both Peprotech) and 1% penicillin/streptomycin.

qRT-PCR

Total RNA was extracted with the phenol-chloroform (both Sigma-Aldrich) method or Arcturus PicoPure RNA extraction kit. First-strand reverse transcription was performed using qScript cDNA supermix (Quanta Biosciences). qPCR was performed using VeriQuest Fast SYBR qPCR Master Mix (Affymetrix) on an Applied Biosciences ViiA 7 Real-Time PCR system (Life Technologies).

In Vitro PAS Staining, LDL and ICG Uptake and CYP3A Activity

Periodic acid-Schiff (Sigma-Aldrich) staining was performed according to the manufacturer's instructions. Uptake of low-density lipoprotein (LDL) into MF-iHeps was measured by imaging the incorporation of fluorescent Dil-ac-labeled LDL (Molecular Probes; 5 µl per well of a 12-well plate) 2 hours after supplementation to the medium. Uptake of indocyanine green (ICG; Cardiogreen, Sigma-Aldrich) from the medium (1 mg/mL) was imaged 1 hour after supplementation, release after 6 hours. CYP3A activity analysis was performed as described for MF-iHeps generated in vivo.

Cell Immunofluorescence

Cells were fixed in 4% paraformaldehyde for 30 minutes at room temperature and washed in PBS 3 x 10 minutes. Cells were permeabilized in 0.5% Triton X-100 (Sigma-Aldrich) in PBS for 30 minutes at room temperature and blocked with 3% BSA in PBS for 30 minutes at room temperature followed by incubation with primary antibodies in 1% BSA at 4ºC overnight and secondary antibodies for 1 hour at room temperature. Nuclei were stained with Hoechst 33258 (Sigma-Aldrich). Images were captured using a QImaging QIClick-F-M-12 camera/Olympus IX71 microscope.

Flow Cytometry

MFs transduced in vitro with AAV6-EYFP for 72 hours were harvested with 0.5% trypsin (Life Technologies) and washed in PBS/0.5% BSA/2 mM EDTA. EYFP fluorescence was analyzed by flow cytometry using an LSRII Flow Cytometer (Becton Dickinson). The EYFP signal was collected in FL1 through a 510/21 nm band pass, 495 nm long pass filter set and propidium iodide (Sigma-Aldrich) for live/dead cell discrimination. Flow cytometry data were analyzed using FlowJo X software (Treestar). Primary liver cells were analyzed by flow cytometry using a BD FACS AriaIII. Within the nonparenchymal liver cell population, MFs were detected based on their vitamin A content with a violet laser at 405 nm using 450/50 nm band pass filter (Mederacke et al., 2015; Mederacke et al.,

2013). Kupffer cells were labeled with an F4/80-PE antibody for 1 hour and detected with a yellow/green laser at 561 nm. Hepatocytes were labeled with OC2-2F8 antibody for 1 hour and PE-conjugated goat anti-rat Ig adsorbed against mouse serum proteins was used as secondary antibody. Hepatocytes were detected with the yellow/green laser at 561 nm. All analyses were done in combination with analysis of the FITC channel at 488 nm to detect ZsGreen-positive cells within the population. Sytox Red (Life Technologies) was used to label dead cells for exclusion.

Antibodies

Primary Antibodies				
Antigen	Species	Dilution	Supplier	Catalog #
Albumin	Goat	1/500	Bethyl	A90-234A
Human albumin	Goat	1/500	Bethyl	A90-129A-9
CK19	Rabbit	1/100	Abbomax	602-670
CD16/32	Rat	1/100	eBioscience	14-0161-86
CD31-PE	Rat	1/20	Biolegend	102408
Desmin	Rabbit	1/100	Thermo Scientific	RB-9014-P0
E-Cadherin	Rabbit	1/500	Cell Signaling	3195
F4/80	Rat	1/100	AbD Serotec	MCA497G
F4/80-PE	Rat	1/100	TONBO Biosciences	50-4801
FAH	Rabbit	1/500	Markus Grompe, OHSU (Tarlow et al., 2014)	
GFP	Chicken	1/200	Abcam	Ab13970
GFP	Goat	1/200	Abcam	Ab6673
HNF4α	Mouse	1/100	Abcam	Ab41898
HNF4α	Rabbit	1/2,000	Abcam	Ab201460
LYVE1	Rabbit	1/200	ReliaTech	103-PA50AG
MUP	Goat	1/200	Cedarlane	GAM/MUP
OC2-2F8	Rat	1/20	Craig Dorrell, OHSU (Dorrell et al., 2008)	
αSMA	Rabbit	1/100	Abcam	Ab5694
αSMA	Goat	1/100	Abcam	Ab21027
αSMA (1A4)	Mouse	1/100	Abcam	Ab7817

Secondary Antibodies					
Species	Reactivity	Fluorochrome	Dilution	Supplier	Catalog #
Donkey	Chicken	Cy3	1/200	Jackson Immunoresearch	703-165-155
Donkey	Goat	Alexa Fluor 488	1/200		705-545-147
Donkey	Rabbit	Alexa Fluor 488	1/200		711-545-152
Donkey	Rat	Alexa Fluor 647	1/200		712-605-150
Donkey	Rabbit	Alexa Fluor 594	1/1,000	ThermoFisher	A21207
Goat	Rat	PE	1/20	BD Biosciences	550767

Primers

Gene name	Forward primer (5'-3')	Reverse primer (5'-3')
Acta2	GTCCCAGACATCAGGGAGTAA	TCGGATACTTCAGCGTCAGGA
Alb	GCAGATGACAGGGCGGAACTTG	AAAATCAGCAGCAATGGCAGGC
Afp	TAACCTGGTGAAGCAAAAGC	TTAAGCCAAAAGGCTCACAC
CMV	ACGCCAATAGGGACTTTCCA	GTTGGAGGCTGGATCGGTC
Col1a1	TAGGCCATTGTGTATGCAGC	ACATGTTCAGCTTTGTGGACC
Col1a2	GGTGAGCCTGGTCAAACGG	ACTGTGTCCTTTCACGCCTTT
Cyp1a2	AAAGGGGTCTTTCCACTGCT	AGGGACACCTCACTGAATGG
CYP3A4	CTTCATCCAATGGACTGCATAAAT	TCCCAAGTATAACACTCTACACAGACAA
Cyp3a11	GACAAACAAGCAGGGATGGAC	CCAAGCTGATTGCTAGGAGCA
Des	GAGAAACCAGCCCCGAGCAAAG	AGCCTCGCTGACAACCTCTCCA
Gapdh	GGAGCGAGACCCCACTAACA	ACATACTCAGCACCGGCCTC
GAPDH	GAAGATGGTGATGGGATTTC	GAAGGTGAAGGTCGGAGTC
Mmp2	CAAGTTCCCCGGCGATGTC	TTCTGGTCAAGGTCACCTGTC
Mmp9	CTGGACAGCCAGACACTAAAG	CTCGCGGCAAGTCTTCAGAG
Mmp10	CCTGTGTTGTCTGTCTCTCCAAGA	CGTGCTGACTGAATCAAAGGAC
Mmp12	CTGCTCCCATGAATGACAGTG	AGTTGCTTCTAGCCCAAAGAAC
Mmp13	CTTCTTCTTGTTGAGCTGGACTC	CTGTGGAGGTCACTGTAGACT
Serpina1a	CACTTCCCCAGACTGTCCAT	AGGGGAGCATTTTCCTCTGT
Timp1	GTGCACAGTGTTTCCCTGTTT	TCCGTCCACAAACAGTGAGTGTCA
Timp2	GGATTCCGGGAATGACATCTAT	CGCCTTCCCTGCAATTAGATA
Tgfb1	CACCGGAGAGCCCTGGATA	TGTACAGCTGCCGCACACA
Tgfbr1	TGGCAGAGCTGTGAGGCCTT	GGGCCCAGAGAAACCCTGGGA
Tgfbr2	GCACCAGGGGCCGGTCTATG	TGGGCTTCCATTTCCACATCCGACT
Trf	TGGCACAGGAACACTTTG	TCCTGCTGATTCCGAATG
Vim	CGGCTGCGAGAGAAATTGC	CCACTTTCCGTTCAAGGTCAAG
AAV-*Foxa1*	ACCCAGATGGCCTCCTCTTC	AAACAAGTTGGGCCATGGTC
AAV-*Foxa2*	CCAGGCCTATTATGAACTCATCC	AAACAAGTTGGGCCATGGTC
AAV-*Foxa3*	TCCCGCTCTCTGCTTAATGC	AAACAAGTTGGGCCATGGTC
AAV-*Gata4*	AGCCACGGAGACATCATCAC	AAACAAGTTGGGCCATGGTC
AAV-*Hnf1a*	ACCCAGATGGCCTCCTCTTC	AAACAAGTTGGGCCATGGTC
AAV-*Hnf4a*	ACGATCACCAAGCAAGAAGC	AAACAAGTTGGGCCATGGTC

SUPPLEMENTAL REFERENCES

Borner, K., Niopek, D., Cotugno, G., Kaldenbach, M., Pankert, T., Willemsen, J., Zhang, X., Schurmann, N., Mockenhaupt, S., Serva, A.*, et al.* (2013). Robust RNAi enhancement via human Argonaute-2 overexpression from plasmids, viral vectors and cell lines. Nucleic Acids Res *41*, e199.

Dorrell, C., Erker, L., Lanxon-Cookson, K.M., Abraham, S.L., Victoroff, T., Ro, S., Canaday, P.S., Streeter, P.R., and Grompe, M. (2008). Surface markers for the murine oval cell response. Hepatology *48*, 1282-1291.

Duarte, S., Baber, J., Fujii, T., and Coito, A.J. (2015). Matrix metalloproteinases in liver injury, repair and fibrosis. Matrix Biol *44-46*, 147-156.

Grimm, D., Lee, J.S., Wang, L., Desai, T., Akache, B., Storm, T.A., and Kay, M.A. (2008). In vitro and in vivo gene therapy vector evolution via multispecies interbreeding and retargeting of adeno-associated viruses. J Virol *82*, 5887-5911.

Grimm, D., Streetz, K.L., Jopling, C.L., Storm, T.A., Pandey, K., Davis, C.R., Marion, P., Salazar, F., and Kay, M.A. (2006). Fatality in mice due to oversaturation of cellular microRNA/short hairpin RNA pathways. Nature *441*, 537-541.

Hayes, B.J., Riehle, K.J., Shimizu-Albergine, M., Bauer, R.L., Hudkins, K.L., Johansson, F., Yeh, M.M., Mahoney, W.M., Jr., Yeung, R.S., and Campbell, J.S. (2014). Activation of platelet-derived growth factor receptor alpha contributes to liver fibrosis. PLoS One *9*, e92925.

Henderson, N.C., Arnold, T.D., Katamura, Y., Giacomini, M.M., Rodriguez, J.D., McCarty, J.H., Pellicoro, A., Raschperger, E., Betsholtz, C., Ruminski, P.G.*, et al.* (2013). Targeting of alphav integrin identifies a core molecular pathway that regulates fibrosis in several organs. Nat Med *19*, 1617-1624.

Huang, P., He, Z., Ji, S., Sun, H., Xiang, D., Liu, C., Hu, Y., Wang, X., and Hui, L. (2011). Induction of functional hepatocyte-like cells from mouse fibroblasts by defined factors. Nature *475*, 386-389.

Huang, P., Zhang, L., Gao, Y., He, Z., Yao, D., Wu, Z., Cen, J., Chen, X., Liu, C., Hu, Y.*, et al.* (2014). Direct reprogramming of human fibroblasts to functional and expandable hepatocytes. Cell Stem Cell *14*, 370-384.

Iwaisako, K., Jiang, C., Zhang, M., Cong, M., Moore-Morris, T.J., Park, T.J., Liu, X., Xu, J., Wang, P., Paik, Y.H.*, et al.* (2014). Origin of myofibroblasts in the fibrotic liver in mice. Proc Natl Acad Sci U S A *111*, E3297-3305.

Junqueira, L.C., Bignolas, G., and Brentani, R.R. (1979). Picrosirius staining plus polarization microscopy, a specific method for collagen detection in tissue sections. Histochem J *11*, 447-455.

Li, M., Jayandharan, G.R., Li, B., Ling, C., Ma, W., Srivastava, A., and Zhong, L. (2010). High-efficiency transduction of fibroblasts and mesenchymal stem cells by tyrosine-mutant AAV2 vectors for their potential use in cellular therapy. Hum Gene Ther *21*, 1527-1543.

Lua, I., Li, Y., Zagory, J.A., Wang, K.S., French, S.W., Sevigny, J., and Asahina, K. (2016). Characterization of hepatic stellate cells, portal fibroblasts, and mesothelial cells in normal and fibrotic livers. J Hepatol *64*, 1137-1146.

Malato, Y., Naqvi, S., Schurmann, N., Ng, R., Wang, B., Zape, J., Kay, M.A., Grimm, D., and Willenbring, H. (2011). Fate tracing of mature hepatocytes in mouse liver homeostasis and regeneration. J Clin Invest *121*, 4850-4860.

Matsushita, T., Elliger, S., Elliger, C., Podsakoff, G., Villarreal, L., Kurtzman, G.J., Iwaki, Y., and Colosi, P. (1998). Adeno-associated virus vectors can be efficiently produced without helper virus. Gene Ther *5*, 938-945.

Mederacke, I., Dapito, D.H., Affo, S., Uchinami, H., and Schwabe, R.F. (2015). High-yield and high-purity isolation of hepatic stellate cells from normal and fibrotic mouse livers. Nat Protoc *10*, 305-315.

Mederacke, I., Hsu, C.C., Troeger, J.S., Huebener, P., Mu, X., Dapito, D.H., Pradere, J.P., and Schwabe, R.F. (2013). Fate tracing reveals hepatic stellate cells as dominant contributors to liver fibrosis independent of its aetiology. Nat Commun *4*, 2823.

Peng, L., Yoo, B., Gunewardena, S.S., Lu, H., Klaassen, C.D., and Zhong, X.B. (2012). RNA sequencing reveals dynamic changes of mRNA abundance of cytochromes P450 and their alternative transcripts during mouse liver development. Drug Metab Dispos *40*, 1198-1209.

Roncoroni, C., Rizzi, N., Brunialti, E., Cali, J.J., Klaubert, D.H., Maggi, A., and Ciana, P. (2012). Molecular imaging of cytochrome P450 activity in mice. Pharmacol Res *65*, 531-536.

Schuppan, D., Ruehl, M., Somasundaram, R., and Hahn, E.G. (2001). Matrix as a modulator of hepatic fibrogenesis. Semin Liver Dis *21*, 351-372.

Sekiya, S., and Suzuki, A. (2011). Direct conversion of mouse fibroblasts to hepatocyte-like cells by defined factors. Nature *475*, 390-393.

Tarlow, B.D., Pelz, C., Naugler, W.E., Wakefield, L., Wilson, E.M., Finegold, M.J., and Grompe, M. (2014). Bipotential adult liver progenitors are derived from chronically injured mature hepatocytes. Cell Stem Cell *15*, 605-618.

Ware, B.R., Berger, D.R., and Khetani, S.R. (2015). Prediction of Drug-Induced Liver Injury in Micropatterned Co-cultures Containing iPSC-Derived Human Hepatocytes. Toxicol Sci *145*, 252-262.
Willenbring, H., Bailey, A.S., Foster, M., Akkari, Y., Dorrell, C., Olson, S., Finegold, M., Fleming, W.H., and Grompe, M. (2004). Myelomonocytic cells are sufficient for therapeutic cell fusion in liver. Nat Med *10*, 744-748.
Zhu, S., Rezvani, M., Harbell, J., Mattis, A.N., Wolfe, A.R., Benet, L.Z., Willenbring, H., and Ding, S. (2014). Mouse liver repopulation with hepatocytes generated from human fibroblasts. Nature *508*, 93-97.
Zolotukhin, S., Byrne, B.J., Mason, E., Zolotukhin, I., Potter, M., Chesnut, K., Summerford, C., Samulski, R.J., and Muzyczka, N. (1999). Recombinant adeno-associated virus purification using novel methods improves infectious titer and yield. Gene Ther *6*, 973-985.